

Articles

Catalyst Site Epimerization during the Kinetic Resolution of Chiral α -Olefins by PolymerizationEndy Y.-J. Min,[#] Jeffery A. Byers, and John E. Bercaw*

Arnold and Mabel Beckman Laboratories of Chemical Synthesis, California Institute of Technology, Pasadena, California 91125

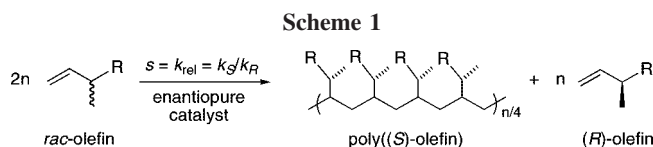
Received July 31, 2007

A new enantiopure C_1 -symmetric olefin polymerization precatalyst, (1,2-SiMe₂)₂{ η^5 -C₅H₂-4-((S)-CHEtCMe₃)}₂{ η^5 -C₅H-3,5-(CHMe₂)₂}ZrCl₂, (**S**)-**2**, was synthesized, and its use for the kinetic resolution of 3-methyl-substituted racemic α -olefins was investigated. Upon activation with methyl aluminoxane (MAO), selectivity factors for most olefins were greater when (**S**)-**2** was used as the catalyst as compared to its previously reported methylneopentyl analogue, (1,2-SiMe₂)₂{ η^5 -C₅H₂-4-((S)-CHMeCCMe₃)}₂{ η^5 -C₅H-3,5-(CHMe₂)₂}ZrCl₂, (**S**)-**1**. Pentad analysis of polypropylene produced by the two catalysts at various propylene concentrations indicates that (**S**)-**2** undergoes more efficient site epimerization (polymeryl chain swinging prior to subsequent monomer enchainment) at intermediate propylene concentrations compared to (**S**)-**1**. At high and low propylene concentrations, however, the two catalysts behave similarly. On the other hand, polymerization of 3,5,5-trimethyl-1-hexene at different olefin concentrations and temperatures illustrated that selectivity differences between the two catalysts are likely not a consequence of inefficient site epimerization for (**S**)-**1**.

Introduction

Polymerizations of α -olefins are among the most rapid and stereoselective of homogeneous catalytic processes.¹ Due to the potential commercial value of the polymers, much effort has been devoted to understanding how catalyst structure affects polymer microstructure. Often there is a direct connection between catalyst symmetry and poly- α -olefin tacticity, with C_2 -symmetric catalysts producing isotactic polymer and C_s -symmetric catalysts producing syndiotactic polymer. As a consequence of these studies, a comprehensive mechanistic picture is being developed for these catalyst systems.²

In principle, the remarkable stereoselectivities displayed by polymerization catalysts could be exploited for the kinetic resolution of racemic α -olefins if enantiopure catalysts are used (Scheme 1).^{3,4} Resolution of simple olefins is generally difficult



because they lack polar directing groups.⁵ For example, asymmetric dihydroxylation of dissymmetric internal olefins can normally be achieved with only modest selectivity,⁶ although in some cases useful selectivities are observed.⁷ A notable alternative to this limitation is the asymmetric alkylation of allylic phosphates, which proceeds in impressive regio- and enantioselectivities.⁸ Kinetic resolution by polymerization has the advantage that isolation of the unreacted olefin product may require only a simple filtration. The enantiopure polyolefins so obtained might also have unique properties.

Due to their exceptionally high activities, the doubly linked enantiopure C_1 -symmetric zirconocene catalyst precursor, (1,2-

* Corresponding author. E-mail: bercaw@caltech.edu.

[#] Current address: Rand Corporation, Santa Monica, CA.

(1) Reviews: (a) Brintzinger, H. H.; Fischer, D.; Mülhaupt, R.; Rieger, B.; Waymouth, R. M. *Angew. Chem., Int. Ed. Engl.* **1995**, *34*, 1143. (b) Britovsek, G. J. P.; Gibson, V. C.; Wass, D. F. *Angew. Chem., Int. Ed.* **1999**, *38*, 428. (c) Coates, G. W. *Chem. Rev.* **2000**, *100*, 1223. (d) Resconi, L.; Cavallo, L.; Fait, A.; Piemontesi, F. *Chem. Rev.* **2000**, *100*, 1253. (e) Wang, B. *Coord. Chem. Rev.* **2006**, *250*, 242.

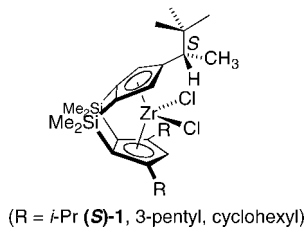
(2) (a) Corradini, P.; Guerra, G.; Vacatello, M.; Villani, V. *Gazz. Chim. Ital.* **1988**, *118*, 173. (b) Corradini, P.; Guerra, G.; Cavallo, L.; Moscardi, G.; Vacatello, M. *Ziegler Catalysts*. In *Ziegler Catalysis, Recent Scientific Innovation and Technological Improvements*; Fink, G.; Mülhaupt, R., Brintzinger, H. H., Eds.; Springer-Verlag: Berlin, 1995; p 237. (c) Guerra, G.; Corradini, P.; Cavallo, L.; Vacatello, M. *Makromol. Chem., Makromol. Symp.* **1995**, *89*, 77. (d) Gilchrist, J. H.; Bercaw, J. E. *J. Am. Chem. Soc.* **1996**, *118*, 12021. (e) Grubbs, R. H.; Coates, G. W. *Acc. Chem. Res.* **1996**, *29*, 85.

(3) Baar, C. R.; Levy, C. J.; Min, E. Y.-J.; Henling, L. M.; Day, M. W.; Bercaw, J. E. *J. Am. Chem. Soc.* **2004**, *126*, 8216.

(4) (a) Ciardelli, F.; Carlini, C.; Altomare, A. *Ziegler Catalysis*; Springer-Verlag: New York, 1995; p 455. (b) Chien, J. C. W.; Vizzini, J. C.; Kaminsky, W. *Makromol. Chem., Rapid Commun.* **1992**, *13*, 479.

(5) Useful methods for the kinetic resolution of functionalized olefins have been accomplished for a variety of functional groups including: allylic alcohols. (a) Gao, Y.; Hanson, R. M.; Klunder, J. M.; Ko, S. Y.; Masamune, H.; Sharpless, K. B. *J. Am. Chem. Soc.* **1987**, *109*, 5765. (b) Martin, V. S.; Woodard, S. S.; Katsuki, T.; Yamada, Y.; Ikeda, M.; Sharpless, K. B. *J. Am. Chem. Soc.* **1981**, *103*, 6237. (c) Kitamura, M.; Kasahara, I.; Manbe, K.; Noyori, R.; Takaya, H. *J. Org. Chem.* **1988**, *53*, 708. Allylic ethers: (d) Adams, J. A.; Ford, J. G.; Stamatou, P. J.; Hoveyda, A. H. *J. Org. Chem.* **1999**, *64*, 9690. (e) Morken, J. P.; Didiuk, M. T.; Visser, M. S.; Hoveyda, A. H. *J. Am. Chem. Soc.* **1994**, *116*, 3123. Allylic acetates: (f) Pamies, O.; Baekvall, J.-E. *Chem. Rev.* **2003**, *8*, 3247. Dienes: (g) La, D. S.; Alexander, J. B.; Cefalo, D. R.; Graf, D. D.; Hoveyda, A. H.; Schrock, R. R. *J. Am. Chem. Soc.* **1998**, *120*, 9720.

$\text{SiMe}_2\{\eta^5\text{-C}_5\text{H}_2\text{-4-}((S)\text{-CHMeCCMe}_3)\}\{\eta^5\text{-C}_5\text{H-3,5-R}_2\}\text{Zr-Cl}_2$ (**(S)-1**), and related precatalysts were initially investigated for the kinetic resolution of 3-methyl-substituted α -olefins (e.g., 3-methyl-1-pentene and 3,4-dimethyl-1-pentene), affording isotactic polymers at all concentrations examined.³



Importantly, this same catalyst system (in its racemic or enantiopure form) effects a gradual change from *syndiotactic* polypropylene to *isotactic* polypropylene as the propylene concentration is reduced.⁹ A switch from *syndiotactic* polypropylene at high propylene concentrations to *isotactic* polypropylene at low propylene concentrations has been reconciled by a competition between bimolecular chain propagation and unimolecular site epimerization, whereby the methyl substituent of the methylneopentyl group pushes the polymer chain to the opposite side of the zirconocene wedge. At low concentrations of propylene, unimolecular site epimerization precedes enchainment of another monomer, and olefin insertion occurs mainly with propylene coordination to the same side of the zirconocene wedge. Because chain propagation occurs using predominately the same enantioface of the olefin, isotactic polymer is produced. At high monomer concentrations, bimolecular chain propagation is relatively favored over site epimerization, thus allowing for propylene enchainments from both sides of the zirconocene wedge with alternating enantiofacial preferences to produce *syndiotactic* polymer.

For hindered 3-methyl-substituted α -olefins, chain propagation is believed to be much slower than site epimerization even at high olefin concentrations. Thus, the blue pathway shown in Scheme 2 dominates and isotactic polymer is produced.

The evidence for isotactic polymer resulting from such polymerizations, however, is largely based on the very high polymer melting points and $^{13}\text{C}\{^1\text{H}\}$ NMR spectra.¹⁰ Unfortunately, these $^{13}\text{C}\{^1\text{H}\}$ NMR spectra, unlike those for polypropylenes, are not particularly diagnostic due to poor polymer solubility and broad overlapping peaks. Consequently, stereoerrors are harder to detect than for polypropylene.

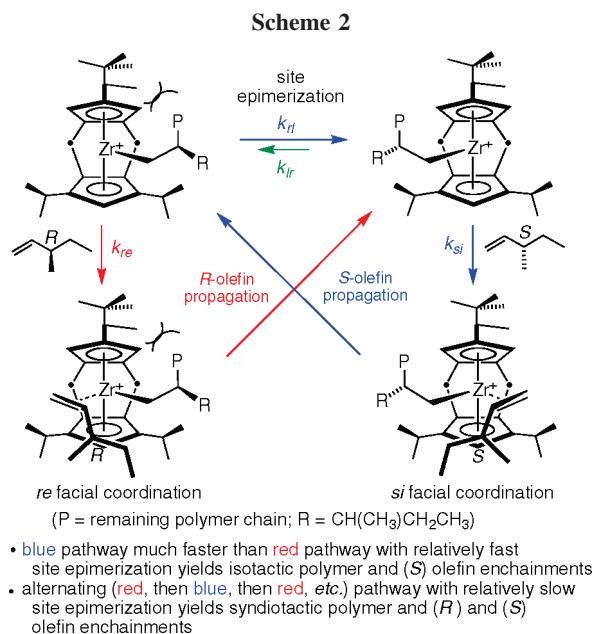
We therefore considered the possibility that low *S* versus *R* monomer selectivities observed during some of the kinetic resolutions are, at least in part, a consequence of inefficient site epimerization, because olefin enchainment when the polymeryl chain lies on the sterically more hindered side of the zirconocene wedge might be expected to result in olefin insertions with opposite monomer enantiofacial and antipode selectivity (Scheme 2). Thus, these misinsertions would be expected to occur with the normally *disfavored* enantiomer of the monomer (*R* for **(S)-1**

(6) (a) VanNieuwenhze, M. S.; Sharpless, K. B. *J. Am. Chem. Soc.* **1993**, *115*, 7864. (b) Hamon, D. P. G.; Tuck, K. L.; Christie, H. S. *Tetrahedron* **2001**, *57*, 9499. (c) Christie, H. S.; Hamon, D. O. G.; Tuck, K. L. *Chem. Commun.* **1999**, 1989.

(7) Gardiner, J. M.; Norret, M.; Sadler, I. H. *Chem. Commun.* **1996**, 2709.

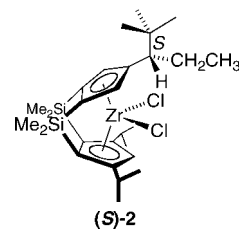
(8) Van Veldhuizen, J. J.; Campbell, J. E.; Giudici, R. E.; Hoveyda, A. H. *J. Am. Chem. Soc.* **2005**, *127*, 6877.

(9) (a) Herzog, T. A.; Zubris, D. L.; Bercaw, J. E. *J. Am. Chem. Soc.* **1996**, *118*, 11988. (b) Veghini, D.; Henling, L. M.; Burkhardt, T. J.; Bercaw, J. E. *J. Am. Chem. Soc.* **1999**, *121*, 564.



along the red pathway), lowering the selectivity for the kinetic resolution by polymerization.¹¹

To examine the possibility that inefficient site epimerization operates with catalyst system **(S)-1**, we have undertaken the synthesis of **(S)-2**. We anticipated that the more sterically demanding ethyl group of **(S)-2** should result in more efficient site epimerization and higher selectivities during the kinetic resolution of racemic α -olefins, as compared with **(S)-1**. In order to further test these assertions, the relative rates of monomer enchainment versus site epimerization for the two catalyst systems were examined by polymerizations of propylene and a chiral α -olefin at various temperatures and olefin concentrations.



Results and Discussion

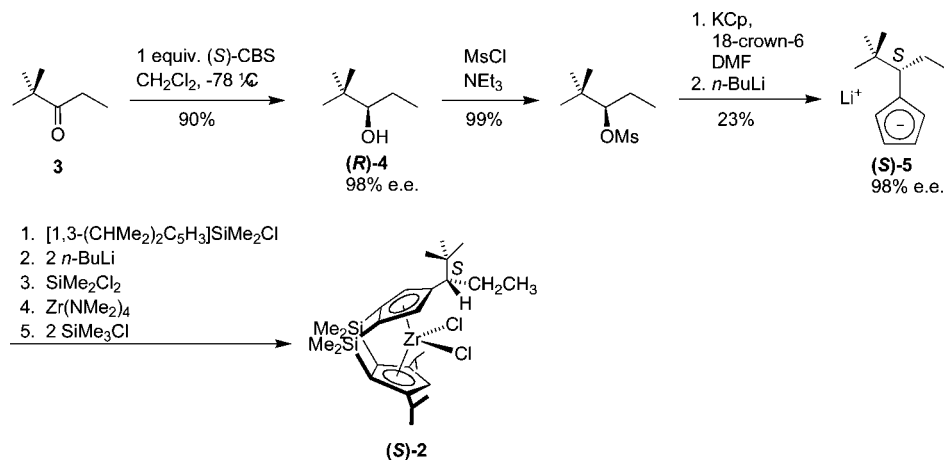
Synthesis of (S)-2 and Polymerization of Racemic α -Olefins. The synthesis of **(S)-2** was carried out as outlined in Scheme 3. This route is analogous to the previously reported synthesis of **(S)-1**,³ but the synthesis of the upper cyclopentadienyl ring (as pictured) deserves some comment. Whereas synthesis of the upper cyclopentadienyl required for **(S)-1** was achieved by CBS reduction of pinacolone, followed by $\text{S}_\text{N}2$

(10) (a) Zambelli, A.; Proto, A.; Pasquale, L. *Zeigler Catalysis*; Springer-Verlag: New York, 1995; p 218. (b) Oliva, L.; Longo, P.; Zambelli, A. *Macromolecules* **1996**, *29*, 6383. (c) Sacchi, M. C.; Barsties, E.; Tritto, I.; Locatelli, P.; Brintzinger, H. H.; Stehling, U. *Macromolecules* **1997**, *30*, 1267.

(11) Although the two stereoisomers of the olefin adducts shown in Scheme 2 are not strictly mirror images, the adduct using the opposite olefin antipode would be the expected favored stereoisomer if steric influence from the isopropyl groups on the lower cyclopentadienyl (as pictured) groups of the ligand predominate and if chain end effects do not dominate. For a study of the relative contributions of site and chain end control, see ref 17.

(12) Enzymatic kinetic resolution of **(R)-4** was also attempted, but the desired alcohol could not be recovered in high yields and optical purities. Min, E. Y.-J. Ph.D. Thesis, California Institute of Technology, 2005.

Scheme 3



displacement of the corresponding mesylate with cyclopentadienyl anion, analogous procedures were problematic for the synthesis of (S)-2. Instead of the 10 mol % *in situ* prepared CBS catalyst, which was used for pinacolone reduction, a stoichiometric amount of solid preformed CBS catalyst was required to reduce **3** to the corresponding alcohol, (R)-4, in high optical purities.¹² Lower temperatures (−78 vs −20 °C) as well as longer addition times were also required to achieve 98% enantiomeric excess. Treating the mesylate of (R)-4 with cyclopentadienyl anion was also more challenging for the synthesis of (S)-5, as compared to the analogous reaction during the synthesis of (S)-1. Although the product of the reaction was obtained with complete inversion of stereochemistry, yields of the enantiopure cyclopentadienyl analogue, (S)-5, were low. In fact, the major product of this reaction was elimination of the mesylate rather than S_N2 displacement. Nevertheless, synthesis of (S)-5 could be accomplished albeit in low yields, and elaboration to (S)-2 was carried out in complete analogy and in similar yields to (S)-1.

An X-ray crystal structure obtained for (S)-2 (Figure 1) reveals similar structural features to (S)-1. The ethyl group occupies the right side of the zirconocene wedge in a similar fashion to the methyl group of (S)-1. The distance between the two isopropyl groups on the bottom cyclopentadienyl ring are 5.124(2) Å for (S)-2 compared to 5.163(2) Å for (S)-1, and the angles between the two cyclopentadienyl ring planes are 73.1° and 72.2° for (S)-2 and (S)-1, respectively. The only major difference between the two structures is the torsional angle between the methyl (methylene of (S)-2) group on the top Cp, the Cp centroid, and zirconium, which is 39.1° for (S)-1 as compared to 46.7° for (S)-2. Other relevant bond distances and angles appear in the Supporting Information.

In the presence of methylaluminoxane (MAO) as cocatalyst, polymerizations of several racemic α -olefins were carried out with (S)-2, and the results are shown in Table 1 along with results from analogous runs with (S)-1 for comparison. In general, (S)-2 was the more active catalyst, possibly due to the slightly more open zirconocene structure for (S)-2 compared to (S)-1. However, care must be taken when interpreting activity for these polymerizations because reaction times were varied significantly in order to achieve appropriate conversions for reliable selectivity factors (50 ± 20%). Because these catalysts are not living, the amount of decomposed catalyst affects activity calculations for polymerizations carried out at different reaction times. Furthermore, because only a fraction of the dissolved catalyst is active for polymerization,¹³ it is likely that the concentration of active catalyst varies depending on the identity of the catalyst, the counterion, and the monomer.

In most cases, the selectivity factors for polymerizations catalyzed by (S)-2 were larger than for (S)-1, a trend that is particularly evident for 3,5,5-trimethyl-1-hexene. The one exception is the polymerization of 3,4,4-trimethyl-1-pentene, which was significantly less selective when (S)-2 was used. We are unsure of the reason for this anomaly, but it could be associated with the lower molecular weights of the polymer produced by (S)-2 compared to (S)-1. Inherent to lower molecular weight polymer are more olefin insertions into [Zr–H], a process that has been shown to have poor enantiofacial selectivity.¹⁴ This hypothesis is supported by the observation of dimers (GC) during polymerizations. Additionally, the polymer that was recovered from these reactions accounted for only 60% (by mass) of the converted olefin for (S)-2 compared to 70% for (S)-1. The remainder of the mass was presumably

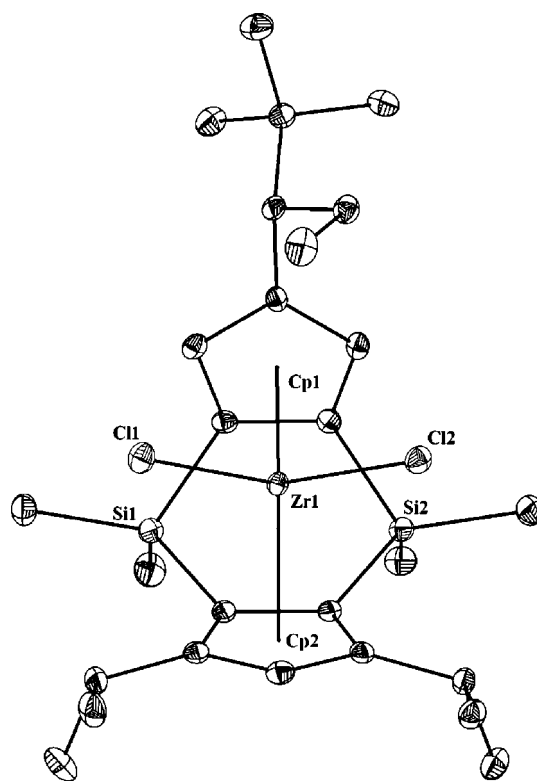
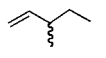
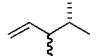
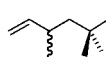
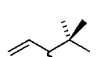


Figure 1. Molecular structure for (1,2-SiMe₂)₂{ η^5 -C₅H₂-4-((S)-CH₂EtCMe₃)}{ η^5 -C₅H-3,5-(CHMe₂)₂}ZrCl₂ ((S)-2). For relevant bond angles and distances see the Supporting Information.

Table 1. Kinetic Resolutions of 3-Methyl-Substituted α -Olefins Using (S)-1 and (S)-2^a

olefin	(S)-1		(S)-2	
	TOF (h ⁻¹)	$s = k_S/k_R$	TOF (h ⁻¹)	$s = k_S/k_R$
	47	2.4	280	3.2
	34	15.9	75	20.5
	37	2.1	988	8.5
	18 ^a	7.6	16 ^a	3.2

^a Polymerizations were carried out at room temperature with 2.0 mL of olefin, 250 mg of MAO (1000 equiv), and 1.5 mL of tetradecane using 1–2 mg of catalyst.

lost during polymer purification as methanol-soluble and/or more volatile oligomers.

Although the substrates represented in Table 1 are limited, and the magnitude of the selectivity enhancement is substrate dependent, improved selectivities are consistent with more efficient site epimerization during polymerization with (S)-2 as compared to (S)-1 (*vide supra*). In order to test this hypothesis, propylene polymerizations, as well as polymerizations of a racemic α -olefin, were carried out at different temperatures and olefin concentrations.

Propylene Polymerizations Catalyzed by (S)-2. As noted above, due to the competition between site epimerization and chain propagation, precatalyst (S)-1 produces moderately syndiotactic polypropylene in neat propylene and moderately isotactic polypropylene at low propylene concentrations.⁹ If (S)-2 undergoes faster site epimerization than (S)-1, then polymers produced from (S)-2 should be more isotactic (lower $[r]$) than polymers produced from (S)-1 at all concentrations of propylene. Propylene polymerizations were therefore carried out at various propylene concentrations, and the tacticities of these polymers were determined by ¹³C NMR spectroscopy. Results from these experiments along with similar experiments carried out with (S)-1 are given in Table 2.¹⁵

As was the case with (S)-1, isotacticity decreased with increasing propylene concentration when (S)-2 was used as the catalyst (e.g., $[mmmm] = 62.3\%$ and 12.9% for $[C_3H_6]$ of 0.8 M and 8.1 M, respectively). Figure 2 shows the dependence of $[r]$ on $[C_3H_6]$ for the two precatalysts (S)-1 and (S)-2. The methyl region of the ¹³C NMR spectra for polypropylenes obtained at three concentrations is shown in Figure 3. As can be seen in Figure 2 both catalysts display saturation behavior at high propylene concentrations. At low propylene concentration ($[C_3H_6] = 0.8$ M), isotactic polypropylene is produced with virtually identical microstructures for the two catalysts (Table 2, entries 1 and 2, and Figure 3), and at high propylene con-

centrations the two catalysts yield syndiotactic polypropylene with similar microstructures (entries 7 and 8). At intermediate propylene concentrations differences between the two catalysts are evident (entries 3–6, Figure 3). Although $[r]$ increases with propylene concentration to similar limiting levels for both catalysts, the increase is more rapid for (S)-1 than (S)-2 (Figure 2, Table 2).

A possible explanation for this behavior is as follows. At the lowest propylene concentration, site epimerization occurs after nearly every olefin insertion for both catalysts, and moderately isotactic ($[r] \approx 14\%$) polypropylene is obtained. The microstructure observed for these polypropylenes, therefore, is largely controlled by the enantiofacial selectivity for olefin insertion when the polymer chain lies on the sterically less hindered side of the zirconocene wedge, and not surprisingly, the enantioselectivities are similar for the two catalysts (*vide infra*). At intermediate propylene concentrations site epimerization competes with olefin insertion for both catalysts. As was expected, the ethyl group of (S)-2 encourages site epimerization more than does the methyl group of (S)-1, and accordingly $[r]$, which is proportional to the number of consecutive olefin insertions without site epimerization, increases more gradually with propylene concentration for (S)-2 (Table 2 and Figure 2). At high propylene concentrations, site epimerization occurs much less often, relative to chain propagation, for either catalyst and $[r]$ approaches a common value of approximately 77%. Polymer microstructure is again controlled by the enantiofacial selectivity for monomer insertions, but under these conditions both sides of the zirconocene wedge are utilized. Given the similar structures for (S)-1 and (S)-2, it is not surprising that these selectivities (and polymer tacticities) are similar. Furthermore, polymerizations carried out in liquid propylene at 0 °C, conditions that minimize the number of site epimerizations relative to monomer enchainments, displayed almost identical polymer microstructures for both catalysts (Table 2, entries 9 and 10; Figure 3).

To quantitatively evaluate how changes in catalyst structure effect polymer microstructure, the pentad distributions for the polypropylenes obtained in liquid propylene were modeled with a three-parameter model¹⁶ that includes (a) α , the enantiofacial selectivity of propylene insertion when the polymeryl group lies on the sterically less hindered side of the zirconocene (having values from 1 to 0), (b) β , the enantiofacial selectivity of propylene insertion when the polymeryl group lies on the sterically more crowded side (having complementary values from 0 to 1), and (c) ϵ , the probability for site epimerization with the polymeryl group moving from the more to the less sterically hindered side (having values from 0 to 1).¹⁷ Thus, a perfectly syndiotactic polypropylene produced with a C_1 -symmetric catalyst would display $\alpha = 1$, $\beta = 0$, and $\epsilon = 0$; a perfectly isotactic polypropylene would display $\alpha = 1$ and $\epsilon = 1$. Least-squares fits of the pentad distributions for polymers made in neat propylene at 0 °C (entries 9 and 10 of Table 2) give $\epsilon = 0.99$ and 0.99 , $\beta = 0.16$ and 0.13 , and $\alpha = 0.13$ and 0.21 (rms = 0.871 and 0.904), for (S)-1 and (S)-2, respectively. Thus, the significantly larger value of ϵ for (S)-2 does indicate that site epimerization is more efficient as compared to (S)-1 even under these conditions where site epimerization is limited.

(13) (a) Liu, Z.; Somsook, E.; Landis, C. R. *J. Am. Chem. Soc.* **2001**, *123*, 2915, and references therein. (b) Klamo, S. B. Ph.D. Thesis, California Institute of Technology, May 2005.

(14) (a) Waymouth, R.; Pino, P. *J. Am. Chem. Soc.* **1990**, *112*, 4911. (b) Longo, P.; Grassi, A.; Pellecchia, C.; Zambelli, A. *Macromolecules* **1987**, *20*, 1015. (c) Sacchi, C.; Barsties, E.; Tritto, I.; Locatelli, P.; Brintzinger, H. H.; Stehling, U. *Macromolecules* **1997**, *30*, 3955.

(15) As we previously observed (ref 3), irreproducible turnover rates and inexplicable differences with changes in catalysts and monomer structure were observed. We therefore do not feel that these experimental conditions are adequate to allow us to extract reliable kinetic parameters for the development of rate laws (e.g., order of reaction in [propylene]).

(16) Miller, S. A. Ph.D. Thesis, California Institute of Technology, Nov 2000.

(17) For other examples of kinetic models used to describe similar situations see: (a) Nele, M.; Mohammed, M.; Xin, S.; Collins, S. *Macromolecules* **2001**, *34*, 3830. (b) deCarvalho, A. B. M.; Gloor, P. E.; Hamielec, A. E. *Polymer* **1990**, *31*, 1294. (c) Farina, M.; Di Silvestro, G.; Sozzani, P. *Macromolecules* **1993**, *26*, 946.

Table 2. Propylene Polymerizations with Precatalysts (S)-1 and (S)-2 at Various [C₃H₆]^b

entry	precatalyst	[C ₃ H ₆] (M)	activity (g _{poly} /(g _{cat} ·h))	[mmmm]	[mnmr]	[rmmr]	[mmmr]	[mrrm] + [rrmr]	[mrrr]	[rrrr]	[mrrr]	[mrrm]	[r]
1	(S)-1	0.8	2.5 × 10 ³	62.9	14.0	0.9	12.7	3.8	0.0	0.0	1.5	4.4	14.1
2	(S)-2	0.8	1.2 × 10 ³	62.3	14.5	0.8	11.8	5.0	0.0	0.0	1.1	4.5	14.0
3	(S)-1	3.4	5.3 × 10 ³	17.7	15.0	3.3	19.9	9.1	0.0	14.6	12.0	8.3	49.4
4	(S)-2	3.4	6.1 × 10 ³	30.7	16.7	2.7	19.2	7.1	0.0	6.8	8.1	8.7	36.8
5	(S)-1	4.6	1.0 × 10 ⁴	9.9	11.6	3.7	18.9	10.3	0.0	23.9	16.2	5.7	60.4
6	(S)-2	4.6	7.2 × 10 ³	21.8	15.7	3.2	20.0	8.4	0.0	11.6	11.1	8.1	45.0
7	(S)-1	8.1	6.8 × 10 ³	8.8	10.1	3.4	16.6	9.5	0.0	29.9	15.9	5.9	64.7
8	(S)-2	8.1	2.0 × 10 ⁴	12.9	13.0	3.5	18.9	10.1	0.0	19.5	15.2	7.0	56.2
9 ^b	(S)-1	12.1	1.5 × 10 ³	4.0	5.4	3.8	12.6	6.8	0.0	49.6	14.4	3.5	77.2
10 ^b	(S)-2	12.1	2.9 × 10 ⁵	2.8	6.4	3.2	11.6	10.0	0.0	44.4	16.4	5.2	76.8

^a Polymerizations were carried out at 20 °C in 20 mL of toluene using MAO (1000 equiv) as the cocatalyst and under constant pressure of propylene.

^b Neat propylene, 0 °C.

Additionally, these best fits reveal that enantiofacial selectivities for enchainments from each of the two sides of the wedge are similar for the two catalysts.

Using α and β from the neat propylene data, the rest of the data in Table 2 can be modeled by least-squares fitting the best values of ε for each polypropylene.^{18,19} Figure 4 shows a plot of ε versus [C₃H₆] for both catalysts. As expected from the above mechanistic arguments, ε decreases with increasing propylene concentration for both catalysts, indicating that site epimerization occurs more readily at low propylene concentration. At intermediate and high propylene concentrations, ε is larger for (S)-2 compared to (S)-1, with changes in ε being more pronounced for (S)-2, consistent with the ethyl group of (S)-2 being more effective at directing the polymeryl group toward the sterically less hindered side of the zirconocene wedge.

The rate constant for site epimerization (k_{epim}) relative to olefin insertion when the polymer chain resides on the sterically congested side of the zirconocenes ($k_{\beta\text{-ins}}$) can be obtained from the data in Figure 4. The probability of site epimerization can be expressed in terms of these rate constants using the simple relationship shown in eq 1 and the double reciprocal relationship in eq 2:

$$\varepsilon = \frac{k_{\text{epim}}}{k_{\text{epim}} + k_{\beta\text{-ins}}[\text{C}_3\text{H}_6]} \quad (1)$$

$$\frac{1}{\varepsilon} = 1 + \frac{k_{\beta\text{-ins}}}{k_{\text{epim}}}[\text{C}_3\text{H}_6] \quad (2)$$

Plots (Figure 5) of $1/\varepsilon$ versus [C₃H₆] for the data of Figure 4 fit reasonably well to the relationship in eq 2 for each catalyst, producing linear plots with y-intercepts equal to 1. In Figure 5, the smaller slope of the plot for catalyst system (S)-2 probably reflects its tendency to undergo site epimerization more rapidly compared to (S)-1, but this is not conclusive because both k_{epim} and $k_{\beta\text{-ins}}$ likely change as the catalyst system is varied. Nevertheless, these data show that (S)-2 encourages site epimerization *relative* to olefin insertion marginally better than (S)-1 for propylene polymerizations.

(18) Modeling the pentad data in Table 2 with three parameters yielded better least-squares fits, as expected, but it is unclear why α and β would vary with propylene concentration. Moreover, α and β are likely more accurate at high propylene concentrations because the syndiotactic polymer so obtained results from enchainments using both sides of the zirconocene wedge.

(19) While it is not strictly correct to use α and β determined from neat propylene polymerizations carried out at 0 °C to describe polymerizations carried out at 20 °C, a reasonable estimate for these parameters can be obtained because a shallow temperature dependence on enantiofacial selectivity was observed for a similar system: Herfert, N.; Fink, G. *Makromol. Chem. Makromol. Symp.* **1993**, *66*, 157.

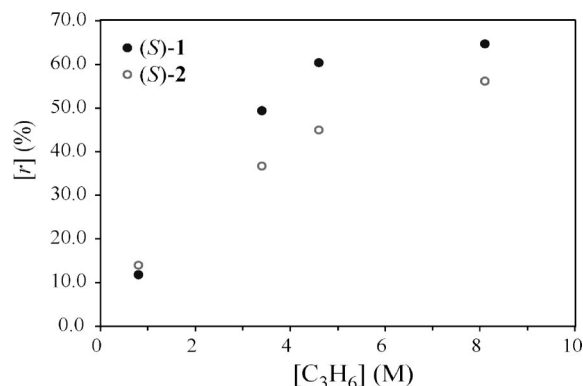


Figure 2. Plot of [r] versus [C₃H₆] for propylene polymerizations catalyzed by (S)-1 and (S)-2.

Polymerization of 3,5,5-Trimethyl-1-hexene at Different Temperatures and Olefin Concentrations. Because chain propagation is known to be much slower for 3-substituted-1-olefins,^{13b} we hypothesized that the 3-methyl-substituted racemic α -olefins used for kinetic resolution would behave much like propylene polymerization at low propylene concentrations; that is, chain propagation would be too slow to compete with site epimerization. If chain propagation, which is first-order in olefin concentration, is in competition with olefin-independent site epimerization during polymerization of racemic α -olefins, then selectivity factors should increase at lower olefin concentrations (*vide supra*). Olefin concentration decreases as the reaction proceeds, so we might expect to observe selectivity factors increase with conversion if site epimerization were in competition with chain propagation. Qualitatively, we have noticed that selectivity factors are insensitive to conversion during racemic α -olefin polymerizations. This observation is not conclusive, however, because olefin concentrations do not vary significantly under typical reaction conditions, where conversions are carried out to 50 ± 20% in order to obtain precise selectivity factors.

We therefore undertook polymerizations of 3,5,5-trimethyl-1-hexene at different initial olefin concentrations using (S)-1 and (S)-2 as precatalysts (Table 3, entries 2, 3, 6, and 7). Curiously, for polymerizations catalyzed by (S)-1 selectivity factors are greater when toluene is used as opposed to tetradecane (compare entry 3 in Table 3 with entry 2 in Table 2). Previously, we reported that selectivity factors for racemic olefins (other than 3,5,5-trimethyl-1-hexene) were insensitive to the solvent used for the reaction.¹¹ At this time we have no explanation for this variance. Nevertheless, the results presented in Table 3 are inconsistent with site epimerization competing with chain propagation because selectivity factors remain the same (for (S)-1) or even slightly decrease (but not significantly so) with decreasing olefin concentration (for (S)-2).

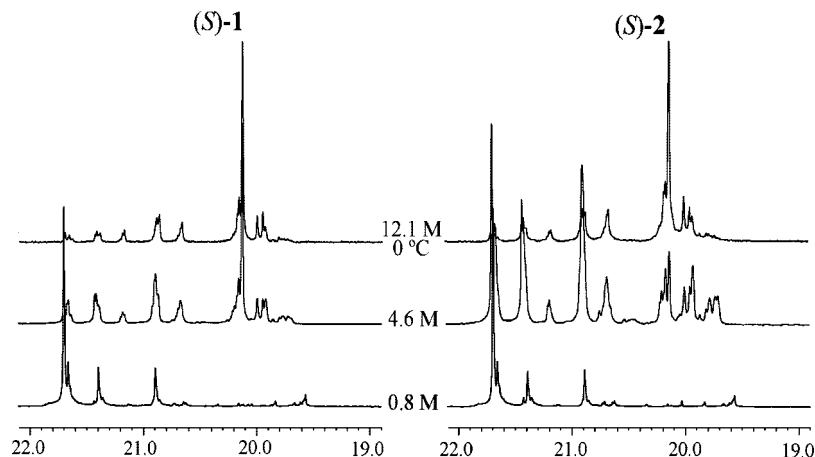


Figure 3. Methyl region of $^{13}\text{C}\{^1\text{H}\}$ NMR for polypropylene polymerized at different $[\text{C}_3\text{H}_6]$ catalyzed by (S)-1 and (S)-2 with methylaluminoxane cocatalyst.

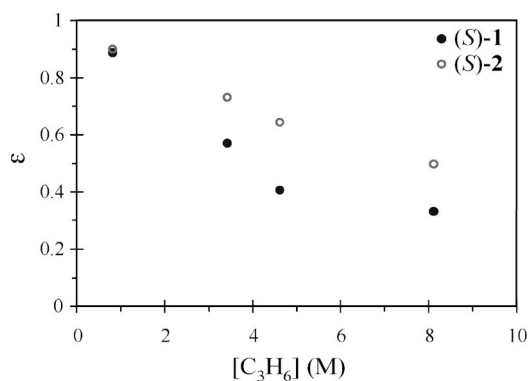


Figure 4. Propylene concentration dependence on the probability of site epimerization parameter (ϵ) obtained by least-squares fits to the data in Table 2.

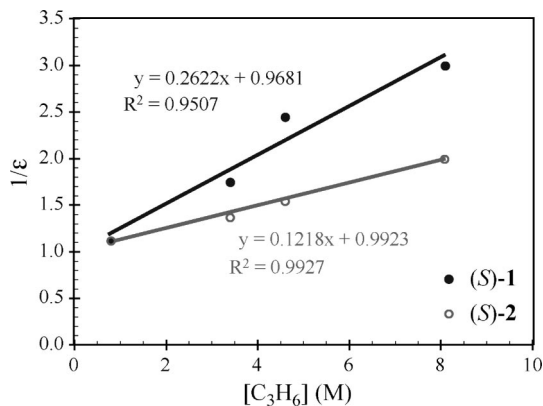


Figure 5. Plot of $1/\epsilon$ versus $[\text{C}_3\text{H}_6]$ for propylene polymerizations catalyzed by (S)-1 and (S)-2.

To complement studies of the effects of olefin concentration on selectivity factors, 3,5,5-trimethyl-1-hexene was polymerized at different temperatures using (S)-1 and (S)-2 as catalysts (Table 3). The results, displayed graphically in Figure 6, clearly show that selectivity decreases with increasing temperature for both catalysts, but more dramatically so for (S)-2. Selectivity factors are expected to be particularly sensitive to temperature, if second-order chain propagation is in competition with first-order site epimerization. Under these circumstances the second-order process, typically characterized by a more negative entropy and lower enthalpy of activation, should be less competitive with the first-order process at higher temperatures. Therefore, site

Table 3. Selectivity and Activity for 3,5,5-Trimethyl-1-hexene Polymerizations Carried Out at Various Olefin Concentrations and Temperatures^a

entry	catalyst	[olefin] (M)	T ($^{\circ}\text{C}$)	TOF (h^{-1})	$s = k_S/k_R$
1	(S)-1 ^b	2.4	0	40 (10)	3.9 (0.2)
2	(S)-1 ^b	0.85	20	110 (30)	2.9 (0.2)
3	(S)-1	2.4	20	110 (30)	3.2 (0.2)
4	(S)-1	2.4	50	1400 (300)	2.6 (0.1)
5	(S)-2 ^b	2.3	0	50 (40)	11.5 (0.5)
6	(S)-2 ^b	0.86	20	100 (10)	5.8 (0.4)
7	(S)-2	2.3	20	90 (70)	8.4 (0.1)
8	(S)-2	2.3	50	420 (30)	4.9 (0.3)

^a Polymerizations were carried out in toluene with MAO (1000 equiv) and 1 μmol of catalyst. Numbers in parentheses indicate average deviation. ^b 3 μmol of catalyst used.

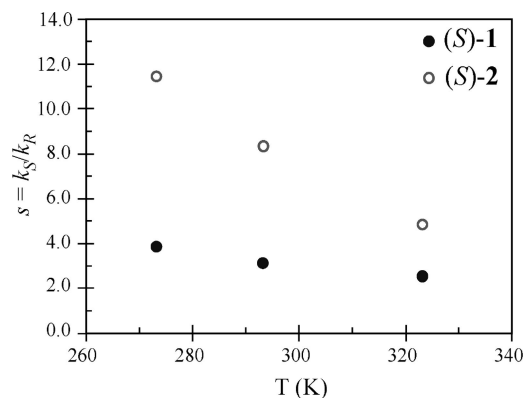


Figure 6. Temperature dependence of selectivity factors (s) during 3,5,5-trimethyl-1-pentene polymerizations catalyzed by (S)-1 and (S)-2.

epimerization should predominate at higher temperatures, and selectivity factors should increase with temperature. The opposite temperature dependence is, in fact, observed for the polymerization of 3,5,5-trimethyl-1-hexene, suggesting once again that chain propagation does not compete with site epimerization for these systems. The explanation for the observed temperature dependence of the selectivity factors is not clear. Perhaps chain end effects, shown earlier to be of substantial importance,²⁰ are particularly temperature dependent for these systems (*vide infra*).

(20) Byers, J. A.; Bercaw, J. E. *Proc. Natl. Acad. Sci.* **2006**, *103*, 15303–15308.

Conclusions

The synthesis of (*S*)-**2** and its use for the kinetic resolution of racemic α -olefins by polymerization revealed enhanced selectivity compared to (*S*)-**1** for most olefins studied. Experiments carried out at varying olefin concentrations demonstrated that, although (*S*)-**2** undergoes more efficient site epimerization than (*S*)-**1** in propylene polymerizations, this mechanism does not account for the difference in selectivities obtained during kinetic resolution of the racemic 3-substituted-1-olefin, 3,5,5-trimethyl-1-hexene. Due to slow insertion rates, it appears that 3-substituted-1-olefins behave similarly to propylene polymerizations at low olefin concentrations where the polypropylene produced from (*S*)-**1** and (*S*)-**2** are indistinguishable.

A possible explanation for the observed differences in selectivity is that chain end control is an important stereodifferentiating factor for (*S*)-**2** and/or (*S*)-**1**. This explanation is particularly attractive because 3,5,5-trimethyl-1-hexene, the olefin that displays the biggest difference in selectivity between the two catalysts, displays different chain end control behavior than the substituted 1-pentenes (i.e., 3,4-dimethyl-1-pentene) when (*S*)-**1** is used as the catalyst.²⁰ Initial ethylene/3,5,5-trimethyl-1-hexene copolymerizations, which probe chain end control by removing the chiral chain with long runs of achiral ethylene comonomer, suggest that chain end control is more important for (*S*)-**2** compared to (*S*)-**1**. For example, when (*S*)-**2** is employed as the catalyst, a copolymerization selectivity factor of 1.7 was observed. Homopolymerization of 3,5,5-trimethyl-1-hexene yields a selectivity factor of 8.0. The corresponding selectivity factors for ethylene copolymerization and homopolymerization catalyzed by (*S*)-**1** are 1.2 and 2.1, respectively.²⁰ Without belaboring this point, it should be emphasized that chiral α -olefin polymerizations involve a pair of diastereomeric pairs per catalytic site (more if one considers chain end control) rather than a pair of diastereomers, as is the case for simple α -olefin polymerization. Selectivity for racemic α -olefin polymerizations should therefore be dictated by matched and mismatched pairs in a double diastereoselective fashion. Our enantiomorphic site control model (Figure 1) includes such double diastereoselective transition state arguments (i.e., the (*S*)-metallocene/*si*-olefin face/(*S*)-olefin diastereomer is favored over the (*S*)/*si*/(*R*) diastereomer), but it is safe to say that the situation is more complex especially when considering the possibility of insertions from both sides of the zirconocene, chain end control, and/or poor enantiofacial selectivity.

Finally, an alternative explanation for the observed differences between (*S*)-**1** and (*S*)-**2** is the contribution of anion reorganization rates during racemic α -olefin polymerization. We believe these factors may affect stereoselectivity during kinetic resolution, and this is an area we are actively investigating.

Modifications of catalysts based on (*S*)-**1** are laborious, as illustrated by the challenges associated with the synthesis of (*S*)-**2**. We are currently exploring C_2 -symmetric zirconocenes and nonmetallocene catalysts for effecting the kinetic resolution of chiral α -olefins by polymerization catalysis.

Experimental Section

General Considerations. All air- and/or moisture-sensitive materials were handled using high-vacuum line, swivel frit assembly, glovebox, Schlenk, and cannula techniques under a nitrogen or argon atmosphere.²¹ Argon was purified by passage through MnO

on vermiculite and activated 4 Å molecular sieves. Propylene (polymer purity, Matheson) was passed through an Oxisorb column (Matheson) before use. All glassware was oven-dried before use.

Solvents were dried and degassed over sodium benzophenone ketyl, calcium hydride, or titanocene.²² Triethylamine, dimethylsilyl dichloride, and trimethylsilyl chloride were stored over and distilled from calcium hydride immediately before use. Unless otherwise mentioned, all starting materials were purchased from Aldrich and used as received. Propionyl chloride was dried over molecular sieves for at least two days before use. Zr(NMe₂)₄ was sublimed before handling in the drybox. (*S*)-**1** and {C₅H-3,5-(CHMe₂)₂}SiMe₂Cl were synthesized as previously reported.³ Dicyclopentadiene was thermally cracked, and the distilled cyclopentadiene was stored at -80 °C until use. 3-Methyl-1-pentene and 3,5,5-trimethyl-1-hexene were purchased from Chemsampco. 3,4,4-Trimethyl-1-pentene and 3,4-dimethyl-1-pentene were prepared as previously described.²⁰ All olefins were dried and degassed over LiAlH₄ for 2 days, then vacuum transferred and stored in Schlenk flasks over CaH₂. In some cases, olefins stored over LiAlH₄ formed into an unusable gel. Methylaluminoxane (MAO) was purchased from Albemarle as 10% or 30% toluene solution. All volatiles were removed *in vacuo* to give a white powder. The white MAO solid was dried at 150 °C for 12 h at high vacuum. Failure to exhaustively dry the MAO in this fashion resulted in surprisingly low selectivity values. Tetradecane was dried over sodium and vacuum distilled into a Schlenk flask, which was stored in the glovebox.

Instrumentation. NMR spectra to characterize compounds were recorded on a Varian Mercury VX300 spectrometer (¹H, 300 MHz; ¹³C{¹H}, 125 MHz). ¹³C{¹H} NMR spectra of polymers were obtained at 100–120 °C on a Varian Inova 500 spectrometer operating at 125 MHz using an acquisition time of 3 s, a relaxation delay of 6 s, a sweep width of 3000 Hz, and a 90° pulse angle. At least 3000 transients were obtained. Conversions for polymerizations were determined by gas chromatography (Agilent 6890) using a 30 m × 0.25 mm polysiloxane “HP-5” column or a 10 m × 0.1 mm “DB-1” column from Agilent Technologies. Enantiomeric excess was determined by gas chromatography (Agilent 6890) using a 30 m × 0.25 mm γ -cyclodextrin trifluoroacetyl “Chiraldex TA” column from Advanced Separations Technology. Elemental analysis was carried out by Desert Analytics and is reported as an average of three independent measurements.

(*S*)-2-Methyl-CBS-oxazaborolidine Borane. (*S*)-2-Methyl-CBS-oxazaborolidine powder (25.0 g, 90.2 mmol) was weighed into a 250 mL round-bottom flask and attached to a swivel frit assembly. Toluene (30 mL) was vacuum transferred onto the white solid. While cooling the white slurry in a -78 °C bath, BH₃·SMe₂ (10.3 mL, 108.2 mmol) was added by syringe through the swivel frit sidearm. The solution was stirred at room temperature for 2 h, then at -10 °C for 5 h. Pentane (180 mL) was vacuum transferred to precipitate out the product. The white slurry was filtered and washed three times with pentane. All volatiles were removed *in vacuo*, and the solid was dried overnight to yield 23.8 g of white powder (91%). ¹H NMR (300 MHz, C₆D₆): δ 0.60 (s, 3H, BCH₃), 0.82 (m, 2H, C4-H₂), 1.24 (m, 2H, C5-H₂), 1.45–2.6 (v br, 3H, BH₃), 2.80 (m, 1H, C6-H), 2.90 (m, 1H, C6-H), 4.38 (t, 1H, C3-H), 6.98 (m, 4H, Ar-H), 7.12 (m, 4H, Ar-H), 7.52 (m, 2H, Ar-H).

2,2-Dimethyl-3-pentanone, 3. A two-neck flask (2 L) equipped with addition funnel (250 mL) and a dry ice condenser was charged with CuCl (~1.5 g). Under argon, propionyl chloride (148.05 g, 1.6 mol) was cannula transferred into the flask. At -78 °C, *tert*-butylmagnesium chloride (2.0 M/Et₂O, 800 mL, 1.6 mol) was added via addition funnel over 2–3 h. The slurry (color can vary from yellow to purple) was allowed to warm to room temperature and stirred for an additional 5 h. At 0 °C, water (500 mL) was added to the reaction mixture. Then 2 N HCl (200 mL) was added to the

(21) Burger, B. J.; Beraw, J. E. *Experimental Organometallic Chemistry*; ACS Symposium Series No. 357; Wayda, A. L., Darenbourg, M. Y., Eds.; American Chemical Society: Washington D.C.; 1987; Chapter 4.

(22) Marvich, R. H.; Brintzinger, H. H. *J. Am. Chem. Soc.* **1971**, *93*, 203.

reaction to dissolve the slurry. The organic layer was washed with 2 N NaOH (200 mL), NaHCO₃ (200 mL), and brine (200 mL), then dried over MgSO₄. The solvent was removed using a rotary evaporator at 0 °C. The yellow oil was distilled at ambient pressure (118–120 °C) to give a colorless liquid (115.31 g, 63%). ¹H NMR (300 MHz, C₆D₆): δ 0.90 (s, 9H, C(CH₃)₃), 0.95 (t, *J* = 7.2 Hz, 3H, CH₃), 2.01 (q, *J* = 7.2 Hz, 2H, CH₂).

(R)-2,2-Dimethyl-3-pentanol, (R)-4. In the drybox, (*S*)-2-methyl-CBS-oxazaborolidine borane was weighed into a round-bottom flask (1 L) equipped with a 180° valve joint. Dichloromethane (300 mL) was vacuum transferred onto the reaction mixture at –78 °C. Under a strong argon purge and while the solution was cooled to –78 °C, 2,2-dimethyl-3-pentanone (dried for 2 days over sieves) (16.53 g, 143.7 mmol) was added by syringe pump over 4 h. The solution was gradually warmed to room temperature, where the reaction stirred overnight. The reaction was quenched by slow addition of methanol (250 mL) at –78 °C. After removing approximately half of the reaction volume by short path distillation, the product was further purified by vacuum distillation using a Vigreux column (30 °C, 1 Torr). A colorless liquid was obtained (15.08 g, 90%). ¹H NMR (300 MHz, C₆D₆): δ 0.82 (s, 9H, C(CH₃)₃), 0.95 (t, *J* = 7.5 Hz, 3H, CH₃), 1.08 (m, 1H, CH₂), 1.25 (d, 1H, OH), 1.34 (m, 1H, CH₂), 2.82 (m, 1H, CH). An ee of 98% was determined for the trifluoroacetate derivative of **4** (GC).

(R)-2,2-Dimethyl-3-pent-1-yl Methanesulfonate. Into a round-bottom flask (500 mL), CH₂Cl₂ (250 mL) and triethylamine (16.0 mL, 0.12 mol) were vacuum transferred. Under an argon purge, (*R*)-**4** (9.3 g, 0.08 mol) (previously dried over sieves for 24 h) was added to the flask by syringe. While cooling at –78 °C, mesyl chloride (10.1 g, 0.088 mol) was added by syringe over 2 min. The slurry was stirred at –78 °C for 1 h, then at room temperature for 1 h, at which time the slurry became yellow. The solution was added to a separatory funnel containing water (200 mL). The organic layer was washed with 1 M HCl (200 mL), saturated NaHCO₃ (200 mL), and brine (200 mL), then dried over MgSO₄. The volatiles were removed to give a dark yellow oil that was unstable at high temperatures (15.43 g, 99%). The product was used without further purification. ¹H NMR (300 MHz, C₆D₆): δ 0.78 (s, 9H, C(CH₃)₃), 0.98 (t, *J* = 7.5 Hz, 3H, CH₃), 1.37 (m, 2H, CH₂), 2.34 (s, 3H, SO₂CH₃), 4.35 (dd, *J* = 7.8, 4.8 Hz, 1H, CH).

(S)-Ethylneopentylcyclopentadienide, (S)-5. In a round-bottom flask (250 mL) equipped with a condenser, potassium cyclopentadienide (33.2 g, 170 mmol) and 18-crown-6 (2.04 g, 8.5 mmol) were dissolved in DMF (40 mL). In a second round-bottom flask (50 mL), (*R*)-2,2-dimethyl-3-pent-1-yl methanesulfonate (16.6 g, 85.4 mmol) was dissolved in DMF (20 mL) and syringed onto the potassium cyclopentadienide solution. The brown solution was heated to 90 °C overnight. At room temperature, the reaction was quenched with water (100 mL). The solution was diluted with hexanes (50 mL). The aqueous layer was isolated and extracted with hexanes (50 mL). The organic layers were combined and washed with 1 M KHSO₄ (50 mL), saturated NaHCO₃ (50 mL), and brine (50 mL), then dried over MgSO₄. The solvent was removed, and the brown oil was Kugelrohr distilled (10^{–3} Torr, 30 °C) to obtain a dark yellow oil composed of (*S*)-**5** and cyclopentadiene dimer (5.34 g, crude yield). The crude product was used without further purification. ¹H NMR (300 MHz, C₆D₆): δ 0.85 (t, *J* = 7.5 Hz, 3H, CH₃), 0.92 (s, 9H, C(CH₃)₃), 1.44 (m, 1H, CH₂), 1.6 (m, 1H, CH₂), 2.07 (dd, *J* = 11.7, 2.7, 1H, CH), 2.78 (br s, 1H, sp³ Cp), 5.95, 6.14, 6.22, 6.30, 6.47 (m's, 4H, sp² Cp). The ee of (*S*)-**5** was determined to be 99% by NMR analysis of the ferrocene derivative.³ [(*rac*)-**5**]₂Fe: ¹H NMR (300 MHz, C₆D₆) δ 0.83 (s, 36H, C(CH₃)₃), 1.17 (t, *J* = 7.5 Hz, 6H, CH₃), 1.18 (t, *J* = 7.5 Hz, 6H, CH₃), 1.66 (m, 4H, CH₂), 1.79 (dd, *J* = 5.7, 2.7, 2H, CH), 1.80 (dd, *J* = 5.7, 2.7, 2H, CH), 2.04 (m, 4H, CH₂), 3.84, 3.96, 3.98, 4.00, 4.04 (m's, 16H, Cp). ¹³C NMR (300 MHz, C₆D₆): δ 17.75 (4C), 25.73, 25.89 (4C), 28.73 (12C), 35.30, 33.34 (4C),

52.12, 52.18 (4C), 67.12, 67.33 (4C), 68.34, 68.40 (4C), 68.54, 68.66 (4C), 71.77, 71.87 (4C), 94.43, 94.65 (4C). The enantiomeric excess of the compound was determined by converting (*S*)-**5** to the corresponding ferrocene, [(*S*)-**5**]₂Fe: ¹H NMR (300 MHz, C₆D₆) δ 0.82 (s, 18H, C(CH₃)₃), 1.18 (t, *J* = 7.5 Hz, 6H, CH₃), 1.66 (quint, *J* = 7.5 Hz, 2H, CH₂), 1.81 (dd, *J* = 5.7, 2.7 Hz, 2H, CH), 2.02 (quint of d, *J* = 7.5, 2.4 Hz, 2H, CH₂), 3.84, 3.99, 4.01, 4.05 (m's, 8H, Cp). ¹³C{¹H} NMR (300 MHz, C₆D₆): δ 17.24 (2C), 25.22 (2C), 28.20 (6C), 34.82 (2C), 51.65 (2C), 66.83 (2C), 68.05 (2C), 68.16 (2C), 71.27 (2C), 93.92 (2C).

Li[(*S*)-ethylneopentylcyclopentadienide]. The round-bottom flask containing the crude (*S*)-ethylneopentylcyclopentadienide was attached to a swivel frit assembly. Ethyl ether (15 mL) was vacuum transferred onto the reaction. At –78 °C, *n*-butyllithium (10.7 mL, 17 mmol) was added via syringe through the sidearm of the swivel frit assembly, and the solution was allowed to stir for 30 min at –78 °C, then at room temperature for 2 h. All volatiles were removed *in vacuo*, and petroleum ether (15 mL) was vacuum transferred onto the white paste. The slurry was filtered and washed with petroleum ether three times. After removing volatiles *in vacuo*, the white solid was dried *in vacuo* overnight to yield 1.72 g (23.4% based on (*R*)-2,2-dimethyl-3-pent-1-yl methanesulfonate). ¹H NMR (300 MHz, THF-*d*₈): δ 0.80 (t, 3H, *J* = 7.5 Hz, CH₃), 0.82 (s, 9H, C(CH₃)₃), 1.52 (m, 1H, CH₂), 1.75 (m, 1H, CH₂), 2.10 (dd, *J* = 11.7, 2.7 Hz, 1H, CH), 3.27 (s, 5.2H, OCH₃), 3.43 (s, 3.9H, OCH₂), 5.51, 5.59 (m, 4H, Cp H).

{C₅H₂-4-((*S*)-CHEtCMe₃)}Me₂Si{C₅H-3,5-(CHMe₂)₂}. In the drybox, Li[(*S*)-ethylneopentylcyclopentadienide] (2.0 g, 11.8 mmol) was charged into a round-bottom flask (100 mL) and connected to a swivel frit assembly. At –78 °C, THF (35 mL) was vacuum transferred onto the mixture, and {C₅H-3,5-(CHMe₂)₂}SiMe₂Cl (2.85 g, 11.8 mmol), dissolved in THF (15 mL), was added portionwise to the reaction. The reaction was slowly brought to room temperature and stirred overnight. The solvent was removed, and petroleum ether (~40 mL) was vacuum transferred onto the reaction mixture, forming a white precipitate. The white precipitate was filtered, and the solvent was removed *in vacuo*, leaving a clear yellow oil. The oil was dried *in vacuo* overnight (4.14 g, 95%). The NMR spectrum was complex due to multiple double-bond isomers, so deprotonation was carried out without further purification or characterization.

Li₂{[C₅H₂-4-((*S*)-CHEtCMe₃)]Me₂Si{C₅H-3,5-(CHMe₂)₂}]DME. Ethyl ether (50 mL) was vacuum transferred onto the oil (4.14 g, 11.2 mmol), which was in a round-bottom flask (100 mL) connected to a swivel frit assembly. At –78 °C, *n*-butyllithium (14.7 mL, 1.6 M in hexane, 23.5 mmol) was syringed onto the solution. The reaction was slowly brought to room temperature overnight. The ethyl ether was removed, and petroleum ether (40 mL) and DME (4 mL) were vacuum transferred onto the reaction mixture. The solution was stirred at room temperature overnight. The white slurry was filtered and washed three times with petroleum ether. All volatiles were removed, and the solid was dried *in vacuo* to obtain an off-white powder (4.7 g, 91%). ¹H NMR (300 MHz, THF-*d*₈): δ 0.30 (s, 12H, SiMe₂), 0.82 (t, 3H, CH₃), 0.82 (s, 9H, C(CH₃)₃), 1.13 (d, 6H, CH(CH₃)₂), 1.14 (d, 6H, CH(CH₃)₂), 1.54 (m, 1H, CH₂), 1.75 (m, 1H, CH₂), 2.10 (dd, 1H, CH(CH₃)₂), 2.78 (h, 1H, CH(CH₃)₂), 3.18 (h, 1H, CH), 3.27 (s, 5.2H, OCH₃), 3.43 (s, 3.9H, OCH₂), 5.66 (m, 3H, C₅H₂), 5.85 (m, 2H, C₅H₃).

(1,2-SiMe₂)₂{C₅H₂-4-((*S*)-CHEtCMe₃)}{C₅H-3,5-(CHMe₂)₂}. Li₂{[C₅H₂-4-((*S*)-CHEtCMe₃)]Me₂Si{C₅H-3,5-(CHMe₂)₂}}·DME (2.61 g, 6.82 mmol) was weighed into a round-bottom flask (250 mL) and affixed to a swivel frit assembly. THF (150 mL) and dimethylsilyl dichloride (0.91 mL, 0.97 g, 7.5 mmol) were vacuum transferred onto the reaction at –78 °C. The reaction was brought to room temperature and allowed to stir at room temperature overnight. The volatiles were removed *in vacuo*. The

resulting oil was triturated once with petroleum ether. A second portion of petroleum ether was vacuum transferred (75 mL) onto the reaction mixture, at which time a white precipitate formed. The precipitate (LiCl) was filtered and washed four times with petroleum ether. The solvent was removed *in vacuo* overnight, leaving a viscous yellow oil (2.07 g, 71%). ¹H NMR (300 MHz, C₆D₆): δ 0.40 (s, 3H, SiMe₂), 0.48 (s, 3H, SiMe₂), 1.20 (s, 3H, SiMe₂), 1.28 (s, 3H, SiMe₂), 1.70 (s, 9H, C(CH₃)₃), ppm (d, 6H, CH(CH₃)₂), (d, 6H, CH(CH₃)₂), 1.95 (t, 3H, CH₃), 2.28 (m, 1H, CH₂), 2.48 (m, 1H, CH₂), 2.92 (m, 1H, CH), 3.32 (h, 1H, CH(CH₃)₂), 3.88 (h, 1H, CH(CH₃)₂), 4.16 (br s, 1H, sp³ Cp H), 4.18 (br s, 1H, sp³ Cp H), 7.10 (br s, 1H, sp² Cp H), 7.68 (br s, 1H, sp² Cp H), 7.85 (br s, 1H, sp² Cp H).

(1,2-SiMe₂)₂{η⁵-C₅H₂-4-((S)-CHEtCMe₃)}{η⁵-C₅H-3,5-CHMe₂)}Zr(NMe₂)₂. In the glovebox, (1,2-SiMe₂)₂{C₅H₂-4-((S)-CHEtCMe₃)}{C₅H-3,5-(CHMe₂)₂} (2.07 g, 4.85 mmol), Zr(NMe₂)₄ (1.30 g, 4.85 mmol), and xylenes (50 mL) were charged in a round-bottom flask (50 mL). The flask was equipped with a condenser and a 180° needle valve joint. On a Schlenk line, the yellow solution was refluxed under a strong argon purge to drive away dimethylamine. The reaction was monitored by placing a wet pH paper at the outlet end of the long needle. When the pH of the reaction was neutral, the reaction was brought to room temperature and all volatiles were removed *in vacuo*. A brown residue was obtained and used in the next step without characterization or further purification.

(1,2-SiMe₂)₂{η⁵-C₅H₂-4-((S)-CHEtCMe₃)}{η⁵-C₅H-3,5-(CHMe₂)₂}ZrCl₂, (S)-2. The flask containing the crude (1,2-SiMe₂)₂{η⁵-C₅H₂-4-((S)-CHEtCMe₃)}{η⁵-C₅H-3,5-(CHMe₂)₂}Zr(NMe₂)₂ (2.9g, 4.85 mmol) was attached to a swivel frit assembly in the drybox. Toluene (40 mL) and trimethylsilyl chloride (10 equiv) were vacuum transferred onto the reaction at -78 °C. The solution was brought to room temperature and stirred overnight. The volatiles were removed, and the product was precipitated out with petroleum ether (20 mL). The precipitate was filtered and washed with petroleum ether until the filtrate was colorless. The solvent was removed and replaced with toluene (20 mL). The precipitate was washed with toluene (10 mL), and the resulting white powder was dried *in vacuo* overnight (0.57 g, 20%). Crystals suitable for single-crystal X-ray crystallography were obtained from a concentrated toluene solution. ¹H NMR (300 MHz, C₆D₆): δ 0.50 (s, 6H, SiMe₂), 0.57, 0.58 (s, 6H, SiMe₂), 0.79 (s, 9H, C(CH₃)₃), 0.97(d, 6H, CH(CH₃)₂), 1.37 (d, 6H, CH(CH₃)₂), 1.41 (m, 3H, EN CH₃), 1.76 (m, 1H, CH₂), 2.47 (coincident multiplets, 2H, EN CH and CH₂), 3.32 (m, 2H, CH(CH₃)₂), 6.49 (s, 1H, C₅H₁), 6.61 (d, 1H, C₅H₂), 6.77 (d, 1H, C₅H₂). ¹³C{¹H} (300 MHz, C₆D₆): δ 165.79, 164.39, 140.12, 137.34, 135.31, 114.51, 114.17, 114.12, 109.64, 109.05, 53.09, 35.64, 29.67, 29.60, 28.70, 28.16, 22.99, 21.00, 20.97, 17.19, 3.72, 3.49, 1.52, 1.46. [α]_D²³ = +5.9 (0.2, THF). Anal Calcd for C₂₇H₄₄Cl₂Si₂Zr: 55.25% C, 7.56% H. Found: 55.2(5)% C, 7.73(2)% H.

Generic Polymerization Procedure for Racemic α-Olefins. MAO (500–1000 equiv) and tetradecane (1.5 mL) were added to a Schlenk flask (10 mL) with a sidearm containing a glass stopcock. The appropriate olefin (1.5–2.0 mL) was vacuum transferred onto the reaction mixture. For reactions in toluene, the solvent was also vacuum transferred onto the reaction (in these cases only a small amount of tetradecane was added to the reaction for an internal standard). The mixture was stirred under argon for a minimum of 30 min. An aliquot was removed via the sidearm for a *t* = 0 reference point. A catalyst stock solution (2 mM) was generally made in toluene or benzene by vacuum transferring the appropriate solvent (3.5 mL) onto the catalyst (5 mg). This solution was used within a few days of preparation. No difference in selectivity or turnover was noticed for older catalyst solutions. The catalyst solution ((1–2) × 10⁻³ mmol) was added by syringe to the reaction vessel via the

sidearm. The reaction mixture generally turned pale yellow. The polymerization was followed by GC by taking occasional aliquots from the reaction (reactions generally take 13–24 h). When the reaction was 30–70% complete, the reaction was stopped by vacuum transferring the remaining volatiles. The MAO was quenched with 10% HCl in methanol (10 mL). The polymer was further purified by precipitation into methanol (200 mL) and stirring overnight. The polymer was dried *in vacuo* at room temperature overnight. Enantioassay was performed by first oxidizing the remaining olefin with RuCl₃(H₂O)₃/NaIO₄ to the carboxylic acid followed by esterification to the methyl ester (BF₃/MeOH) as previously described.³ The methyl ester derivatives could be separated by chiral GC to get enantiomeric excess. The results that appear in Tables 1 and 3 are an average of at least two experiments with the average variance appearing in parentheses.

Polymerization of Racemic α-Olefins at T = 0 °C. The procedure is the same as the generic polymerization procedure except that the reaction was equilibrated at 0 °C with a circulating bath prior to the *t* = 0 GC aliquot, and toluene was used as the internal standard. Catalyst loadings were also higher for these polymerizations ((3–4) × 10⁻³ mmol in 0.5 mL of benzene).

Polymerization of Racemic α-Olefins at T = 50 °C. The procedure is the same as the generic polymerization procedure except a Schlenk tube (50 mL) without a sidearm was used. This change was made to avoid olefin loss at elevated temperatures. Unfortunately, this change also precludes following the reaction by multiple aliquot removal for fear that olefin evaporation would be significant. Additionally, the catalyst solution (1 × 10⁻³ mmol) was introduced to the reaction at ambient temperatures via the Teflon stopcock of the Schlenk tube, then rapidly brought to 50 °C, where it stirred for 2–4 h.

Polymerization of Propylene in Toluene Solutions. MAO (250 mg, ~1000 equiv) and toluene (20 mL) were added to a glass reactor (125 mL, Andrews Glass Co, max. pressure 200 psig) equipped with a septum port, a three-way valve connected to a quick disconnect, a large stir bar, and a pressure gauge (0–300 psig). *CAUTION: this procedure should be performed behind a blast shield.* The flask was connected to the propylene tank and purged with propylene at pressures slightly greater than 1 atm for 5 min. The flask was pressurized to the appropriate pressure of propylene²⁴ for 15 min prior to catalyst injection. A catalyst stock solution (2 mM) was made in the glovebox by dissolving the catalyst (5 mg) in toluene (3.5 mL). This solution was used within a few days and was stored at -30 °C in the glovebox. No differences in activity or tacticity were noticed for polymerizations run with older catalyst solutions. An aliquot of the stock solution (0.5 mL, 1 × 10⁻³ mmol) was loaded in a 1 mL gastight syringe equipped with a long 18-gauge steel needle. The needle was stopped with a septum, and the needle was brought out of the glovebox. The catalyst solution was injected via the septum port against the propylene pressure of the reaction. The reaction was run open to the propylene tank at the appropriate pressure with rapid stirring (700 rpm). The reaction was run for 10–30 min depending on the propylene pressures, with lower propylene pressures requiring longer reaction times. The polymerization was stopped by slowly releasing the excess propylene pressure. The MAO was quenched by slow addition of 10% HCl/MeOH (20 mL). After stirring for 30 min, the polymer was further purified by precipitation into methanol (400 mL). This mixture was allowed to stir a few hours to dissolve all of the aluminoxane. The polymer was isolated by filtration and washed with fresh methanol (3 × 10 mL). The polymer was dried *in vacuo*

(23) Hahn, C.; Cucciolito, M. E.; Vitagliano, A. *J. Am. Chem. Soc.* **2002**, *124*, 9038.

(24) Propylene concentrations were estimated from: Frank, H. P. *Öster. Chem. Zeit.* **1967**, *11*, 360.

at 110 °C overnight. The polymer microstructure was determined by $\{^1\text{H}\}^{13}\text{C}$ NMR (1,1,2,2-tetrachloroethane- d_2 , 110 °C).

Polymerization of Propylene in Neat Propylene ($T = 0$ °C). The procedure was the same as for polymerizations carried out in toluene solutions except only 3 mL of toluene was initially loaded into the reaction vessel. Propylene (~20 mL) was condensed into the reaction vessel at 0 °C. The reaction was maintained at 0 °C with an ice bath. The reaction was run for 10 min before quenching as outlined above.

Acknowledgment. This work was supported by USDOE Office of Basic Energy Sciences (Grant No. DE-FG03-85ER13431) and the National Science Foundation (Grant No. CHE-0131180). We thank Professors Steve Miller and Jay

Labinger for help with the statistical modeling of polymerizations of propylene with catalysts (**S**)-**1** and (**S**)-**2**. We would also like to thank Dr. Larry Henling and Dr. Mike Day for their work in solving the X-ray crystal structure of (**S**)-**2** and Steven Baldwin for help with the characterization of some of the compounds.

Supporting Information Available: X-ray crystallographic data (CIF) and fits from the unimolecular site epimerization model used to model polypropylene pentads. This material is available free of charge via the Internet at <http://pubs.acs.org>.

OM700778E